D1.1 | Co/Al2O3/Al/EuS films

Author(s): Max Ilyn and Celia Rogero

Delivery date: 28.8.2019
Version: 7.0

This project has received funding from the European Union's Horizon 2020 research and innovation programme under grant agreement No 800923.

Project Acronym:	SUPERTED
Project Full Title:	Thermoelectric detector based on superconductor-ferromagnet heterostructures
Call:	H2020-FETOPEN-2016-2017
Topic:	FETOPEN-01-2016-2017
Type of Action:	RIA
Grant Number:	800923
Project URL:	https://superted-project.eu/

Editor:	Max Ilyn, CFM-CSIC; Celia Rogero, CFM-CSIC
Deliverable nature:	Report (R)
Dissemination level:	Public (PU)
Contractual Delivery Date:	31.8.2019
Actual Delivery Date :	28.8.2019
Number of pages:	15
Keywords:	S/FI bilayers, tunnel junctions, temperature, superconducting, pattern, multilayer
Author(s):	Max Ilyn, CFM-CSIC Celia Rogero, CFM-CSIC
Contributor(s):	Carmen González Orellana, CFM-MPC foundation Tero Heikkilä, JYU Heli Lehtivuori, JYU
External contributor(s):	Hisakazu Matsuki, University of Cambridge, UK Kun-Rok Jeon, University of Cambridge, UK Chiara Ciccarelli, University of Cambridge, UK Jason Robinson, University of Cambridge, UK

Abstract

This Deliverbale 1.1 '*Co/Al2O3/Al/EuS*' summarizes the results of the first 12 months of the project (September 2018 – August 2019) on optimization of the growth of multilayer devices. As mentioned in the project proposal, our aim has been to optimize the growth of ferromagnetic insulator/superconductor (S/FI) bilayers. The plan in Work package 1 included the investigation on the fabrication of patterned tunnel junctions based on Al/EuS bilayers in order to produce measurable multilayer structures, *e.g.* Co/Al2O3/Al/EuS and Al/Al2O3/Al/EuS. Main objectives achieved during this period have been the investigation of the properties of EuS films and Al/EuS bilayers as a function of the growth conditions, identifying the importance of growth parameters on the stoichiometry, morphology, and magnetic domain structure of EuS. Finally, we worked towards fabricating Al/EuS-based tunnel junctions, in particular, we focus on Al/Al_2O_3/Al/EuS, to study the exchange splitting of Al electronic states and the magnetoelectric properties. Through systematic research, we can establish an unambiguous relation between desired device properties and the

This project has received funding from the European Union's Horizon 2020 research and innovation programme under grant agreement No 800923.

structural, magnetic, and coupling multilayer properties. However, we have not yet reached the possibility of directly accessing spin splitting in a tunneling current measurement.

This project has received funding from the European Union's Horizon 2020 research and innovation programme under grant agreement No 800923.

1. Properties of the EuS films and Al/EuS bilayers as a function of the growth conditions

The main aim of Work package 1 (WP 1) is the growth of patterned junctions of multilayer thin-film structures containing ferromagnetic insulators and superconductors in the framework of the development of a novel thermoelectric detector. Thermoelectric effect occurs in Superconductor/Normal metal (S/N) tunnel junctions if they satisfy two requirements [1]:

1. The peaks of electronic Density of States (DOS) of a superconductor are split in energy for the two opposite projections of the spin, and
2. Tunnel current is spin-polarized

This latter condition is fulfilled if either a non-superconducting electrode or an insulating barrier is ferromagnetically ordered. Achieving of a spin-split DOS takes the application of an external magnetic field or requires contacting a superconducting electrode with a Ferromagnetic Insulating (FI) material. Therefore, a multilayer structure suitable for generating thermoelectric voltage without an external magnetic field should include a FI/S bilayer.

The material combination selected in this SUPERTED project to produce the FI/S bilayer in the thermoelectric detector is superconducting aluminum (Al) and magnetic semiconductor Europium sulfide (EuS). Al/EuS-based tunnel junctions have recently been used to demonstrate the thermoelectric effect [2] and the existence of the spin-split DOS in these bilayers in the case where the external magnetic field is zero [3]. The lack of information in bilayer preparation conditions makes the reproducibility very difficult [2, 4]. In fact, only one group in the world have succeeded in manufacturing a multilayer system, and there is no a systematic study to compare the growth, crystallinity and magnetic properties of the FI/S junctions.

Previous work on spin-dependent tunneling in Al/EuS-based tunnel junctions revealed several important properties of the system. First, a clean interface between the FI and S layers was found to be crucial for obtaining a spin-split DOS via exchange coupling [5]. It was found that a 2 nm thick layer of the non-magnetic insulator alumina (Al_2O_3) introduced between the FI and S films completely canceled splitting of the electronic DOS of Al [5]. Second, exchange coupling between Al and EuS appeared to be strong enough to destroy the superconducting state in Al. More precisely, the phase transition between a superconducting and normal states in Al/EuS triggered by application of the external magnetic field revealed that a critical value of the field in some cases was comparable to the coercive force of the EuS. Therefore, it was concluded that the main effect of the field consisted in aligning of the magnetic domains of the EuS that increased the interaction strength to the critical level, sufficient for breaking of the superconducting state [5]. Third, the effective field, which is a measure of the strength of the exchange coupling between EuS and Al, was found to be inversely proportional to the thickness of the Al film, if it was not thicker than the superconducting coherence length ξ [5, 6]. Finally, the effective field generated to the exchange coupling between Al and EuS and a zero-field splitting of DOS were sample-specific [5-7].

This project has received funding from the European Union's Horizon 2020 research and innovation programme under grant agreement No 800923.

Main objective of these first 12 months of research was to identify the missing information and to develop a method for growing Al/EuS bilayers with desirable properties [3]. Thus, the aim has been to control systematically the growth parameters and to determine the influence of these parameters on the magnetic properties. We have analyzed how the magnetic properties of EuS films depend on the preparation parameters and how they define the strength of the exchange coupling to Al. This feature together with the dependence of the exchange coupling on the thickness of the Al layer opens up a way to tune the strength of the interaction.

2. EuS film growth

All samples studied in this work were prepared and characterized structurally and chemically in a Ultra High Vacuum (UHV) system (base pressure better than $5x10^{-10}$ mbar). This is a remarkable difference from earlier works. First, although the use of UHV was not a prerequisite for making the Al/EuS bilayers (most of earlier works were done in High Vacuum chambers, base pressure better than $5x10^{-8}$ mbar), we have found that non-optimal vacuum conditions are favorable for the sample/interface contamination and the formation of Eu_2O_3 or other EuS phases, which damages the exchange coupling. Second, this experimental approach allows the sample (structural and chemical) characterization without exposing it to air.

EuS and Al were evaporated from e-beam-heated crucibles. The chemical composition and the structure of the surface crystal were studied by X-ray Photoelectron Spectroscopy (XPS) and Low Energy Electron Diffraction (LEED). Ex-situ measurements of magnetic properties were performed in Quantum Design PPMS system, and Atomic and Magnetic Force Microscopes (AFM, MFM) were used to characterize the surface morphology.

The growth on different substrates and parameters (substrate temperature, flux rate, vacuum conditions) was studied by establishing the relationship between the layer thickness, quality, composition, etc. and the final magnetic response.

2.1 Polycrystalline films of EuS on the SiO2/Si substrate

Following the device scheme in previous studies, we started by testing the growth of EuS directly on SiO_2 [3]. Using XPS overview spectra, we determined the optimal evaporation conditions based on the correct sublimation temperature and correct sample position to obtain layers without impurities (only Eu and S atoms can be detected) and with the correct 1:1 Eu:S ratio on average. In addition, by analyzing high-resolution core level spectra, we detected compositional differences associated with the substrate. For example, the left panel in Fig. 1 shows XPS data acquired in the region of binding energies covering the Eu 3d states.

The spectra shown in Fig. 1a correspond to two samples having the same EuS thickness, 2.6 nm, but deposited on a standard SiO_2 100 nm/Si wafer at different temperatures, 100 K (red spectrum) and 300 K (black spectrum). It is clear that the spectra showed two main peaks, as expected for the two spin-orbit split Eu 3d states ($3d_{3/2}$ and $3d_{5/2}$). However, the positions of these components are

This project has received funding from the European Union's Horizon 2020 research and innovation programme under grant agreement No 800923.

shifted depending on the preparation conditions. The shifts indicate the presence of both Eu^{2+} and Eu^{3+} components and are indicated by dashed lines in Fig 1a.

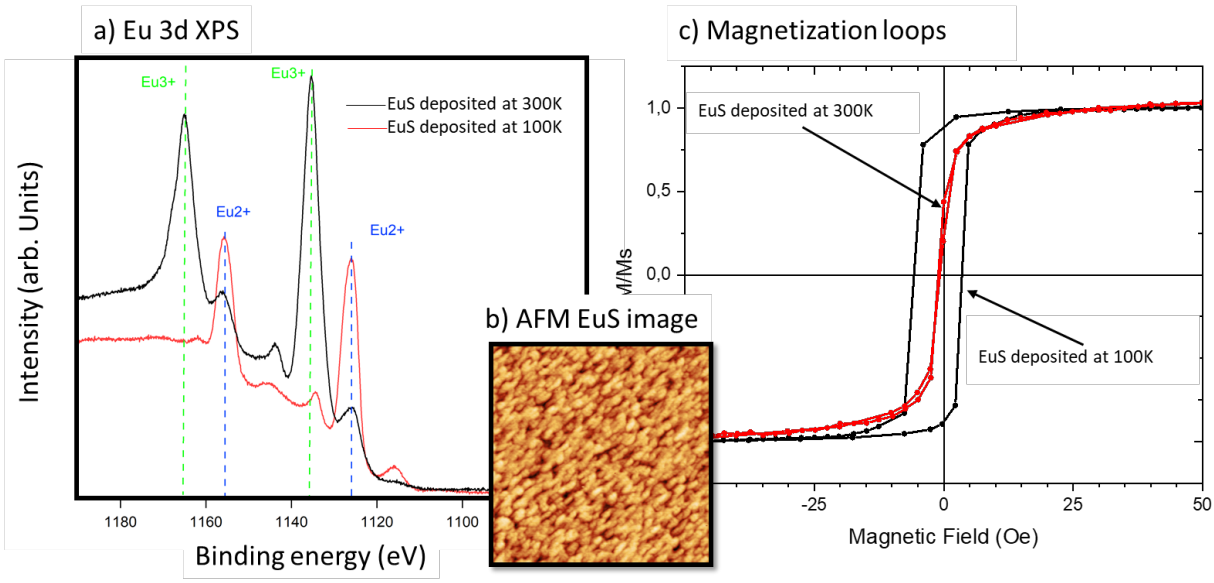

Figure 1: Eu 3d XPS spectra (a) and magnetization loops (c) measured for two samples having the same nominal composition Al(26 nm)/EuS(2.6 nm)/SiO_2/Si but deposited with substrates at different temperature, 100 K and room temperature, respectively. Inserted 1x1 μm^2 AFM image (b) was measured for EuS 15nm/SiO2/Si and the RMS roughness is 0.75 nm.

The stoichiometric EuS should contain only Eu^{2+} ions with high value of the spin moment S=7/2 and zero orbital moment. The spectrum of EuS deposited at room temperature (RT) clearly shows a high contribution of Eu^{3+} ions, which have lower spin moment S=3, orbital moment L=2 antiferromagnetically coupled to the spin moment and overall small total magnetic moment [8]. These results, together with the absence of oxygen signal, suggest the formation of other chemically stable phases, such as Eu_2S_3 or Eu_3S_4. To solve this problem, we changed the "substrate temperature" parameter by cooling down the temperature in the deposition process [9]. As a result, the Eu 3d XPS core level measured for 2.6 nm thick EuS film on oxidized Si wafer pre-cooled with liquid nitrogen shows a significant reduction in the amount of the Eu^{3+} component and thus a better interface stoichiometry. Raising the temperature has no purpose in this project as the surface roughness of EuS increases with increasing temperature, which is a serious obstacle if a continuous thin layer of Al should be grown to the top of EuS layer. AFM surface topography images reveal that, although polycrystalline EuS films are grown, the surface roughness is low enough (RMS roughness is 0.75nm) to be able to grow good Al layers on top (Fig. 1b).

Al-coated samples were used to perform ex-situ magnetic measurements. Figure 1c shows the magnetization loops measured at 5 K for the samples prepared at the two different substrate temperatures mentioned above. Measured magnetization loop for the samples grown at low temperature is similar to the one reported in the work [10] while samples grown at RT have no

This project has received funding from the European Union's Horizon 2020 research and innovation programme under grant agreement No 800923.

hysteresis at 5 K. As a further confirmation, temperature dependent measurements revealed that the Curie temperature (T_C) for RT-grown samples was lower than the temperature at which the hysteresis loops were obtained. The sample prepared at 100 K had a T_C of 7 K, similar to the value previously reported in the literature [10].

These samples were sent to our partners to CNR, Pisa, Italy to measure the sheet resistance of the continuous Al layers. The results are included in the Deliverable 2.1 '*DOS measurements*'. Samples grown at 100 K and at RT are referred in Deliverable 2.1 to as sample 5 (Al(26 nm)/EuS(2.5 nm)/SiO_2) and sample 9 Al(26 nm)/EuS(2.6 nm)/SiO_2), respectively. In addition, we have provided a sample in which the Al film is between two EuS films referred to as sample 12 (EuS(5.14 nm)/Al(18 nm)/EuS(2.7 nm)/SiO2)). Experimental data are presented in Deliverable 2.1, thus only brief conclusions are given here. In both bilayer Al/EuS samples Al was found to be superconducting at low temperatures. Nevertheless, magnetoresistance measurements do not have any features that should accompany the magnetization reversal in the magnetic EuS layers. We believe that the interaction between the thin (2.6 nm) layer of EuS and relatively thick (26 nm) layer of Al is too weak to produce spin-split states in the whole Al film. However, Al film of the same thickness sandwiched between two EuS layers had no superconducting transition below 25 mK. This result could be interpreted as a quenching of the superconductivity by strong exchange coupling to the ferromagnetic layers, but non-reproducible critical temperature of the superconducting transition in the bilayer samples (1.7 K and 2.3 K) raised doubts about the quality of the Al layer. It is known that some amount of impurities increases a temperature of the superconducting transition and if the concentration of impurities is too high, the superconductivity is completely suppressed.

To clarify this issue, a new set of samples has been prepared and sent to Pisa for characterization (referred to as second generation of the samples). Al growth conditions were refined to ensure a clean preparation, e.g. the growth rate was increased and a base chamber pressure improved. As a result, two bilayer Al/EuS samples demonstrated reproducible superconducting transition at 1.7 K. Furthermore, the thickness of the EuS layers was increased to 5 nm and a thickness of Al layer was decreased to 20 nm to enhance the effect of the exchange coupling between superconducting and ferromagnetic layers. In these optimized samples, the magnetoresistance has features at the values of the field equal to the coercive force of the EuS layers and has field hysteresis (see Deliverable 2.1 '*DOS measurements*'). This behavior indicates that magnetic coupling between the EuS and Al affects the resistivity of the superconducting Al film. Finally, the EuS(20 nm)/Al(4 nm)/EuS(6 nm) trilayer sample, with an additional 20 nm thick layer of EuS, did not show superconducting transition down to 25 mK but demonstrated some features that can be interpreted as residual superconductivity. Therefore, we believe that superconductivity in this sample was quenched by a strong exchange coupling to two adjacent ferromagnetic layers. The variation of the exchange coupling strength with the thickness of the ferromagnetic layer led us to perform a detailed study of the magnetic properties of EuS as a function of film thickness.

This project has received funding from the European Union's Horizon 2020 research and innovation programme under grant agreement No 800923.

2.2 Crystal growth of EuS on the InAs(001) substrate

As we mention above, growth on SiO_2 results in polycrystalline films. To determine whether magnetic and exchange coupling properties depend on crystallinity, EuS films were grown on a single crystal semiconductor substrate. We chose InAs(001) because the epitaxial growth of the EuS films has been reported on these semiconductor substrates [11, 12]. Figure 2a shows a comparison of the Eu 4d core level measured on a 2 nm EuS film on InAs(001) grown at RT and the one measured on SiO_2 after deposition at a low temperature (LT). Our first important result was that the high-resolution Eu 4d XPS core level showed no trace of Eu^{3+} component on samples grown on InAs deposited on the substrate at RT. In addition, LEED patterns (not shown) proved that EuS grows epitaxially on InAs(001) at RT [11], and AFM images, Fig. 2b, reveal that the surface is very smooth with a RMS roughness lower than 0.5 nm.

Magnetization loops acquired for Al-coated 2 nm EuS film on InAs(001) sample are shown in Fig. 2c together with the loops of the samples grown at the oxidized Si wafers. Similar to the sample grown on SiO_2 at low temperature, EuS/InAs sample is ferromagnetic with high remanence and demonstrates a higher coercive field, probably due to the higher Curie temperature (T_C of EuS 2nm /InAs is 9 K and T_C of the LT EuS 2.6 nm /SiO_2/Si is 7 K).

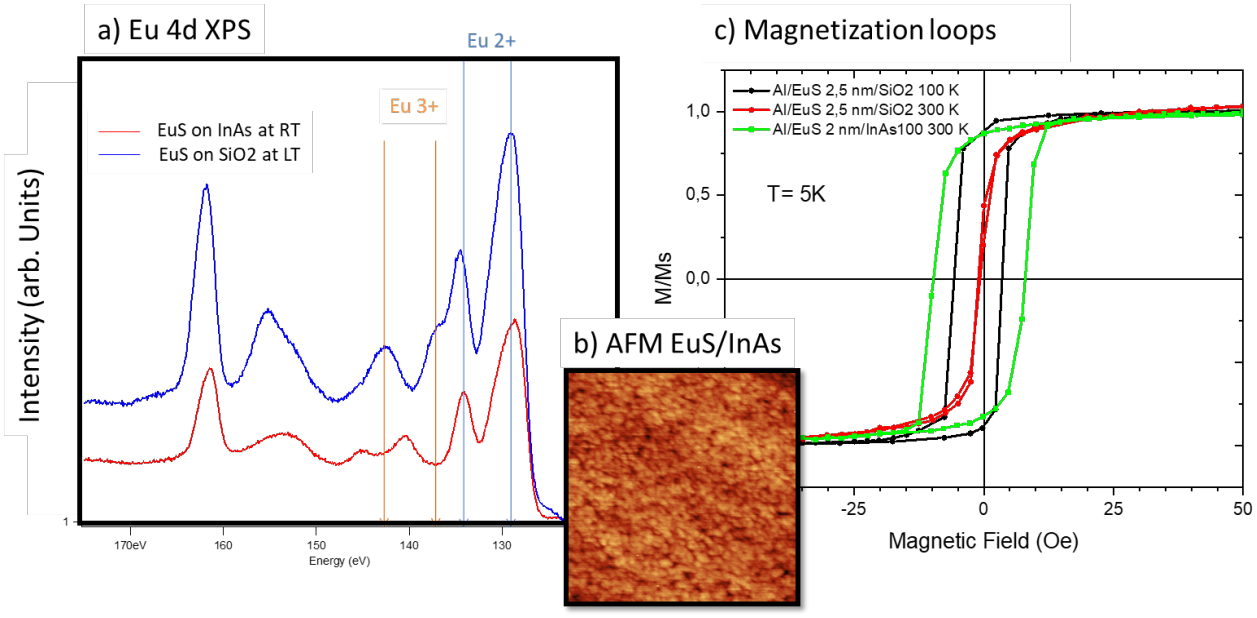

Figure 2: Eu 4d XPS spectra (a) and magnetization loops (c) measured for two samples having similar thickness of the EuS layer but grown on different substrates. The composition of samples is Al(26 nm)/EuS(2.6 nm)/SiO_2/Si and Al(16 nm)/EuS(2 nm)/InAs(001) Inserted 1x1 µm^2 AFM image (b) measured for EuS 15nm/InAs(001) films and the RMS roughness is 0.5 nm.

This project has received funding from the European Union's Horizon 2020 research and innovation programme under grant agreement No 800923.

Characteristic property of the epitaxial EuS/InAs(001) films is the relatively low damping, which allows the use of low-temperature Ferromagnetic Resonance technique (FMR). A major advantage of this method is its ability to determine the precise values of the saturation magnetization of the films. Results of the measurements performed by the group of Dr. J. Robinson (Cambridge University, UK) for the series of the Al-coated EuS/InAs(001) samples shows that the Saturation Magnetization (Ms) has a clear dependence on EuS thickness. Table 1 summarizes these data. It is clearly seen that only a 23 nm thick film demonstrates a saturation magnetization approaching the value of the bulk EuS (Ms bulk is 15.6 kG [8]) meanwhile, the values of Ms for the thinner films are substantially lower. In addition, T_C obtained from temperature-dependent ac-susceptibility measurements (not shown) also increases with increasing thickness.

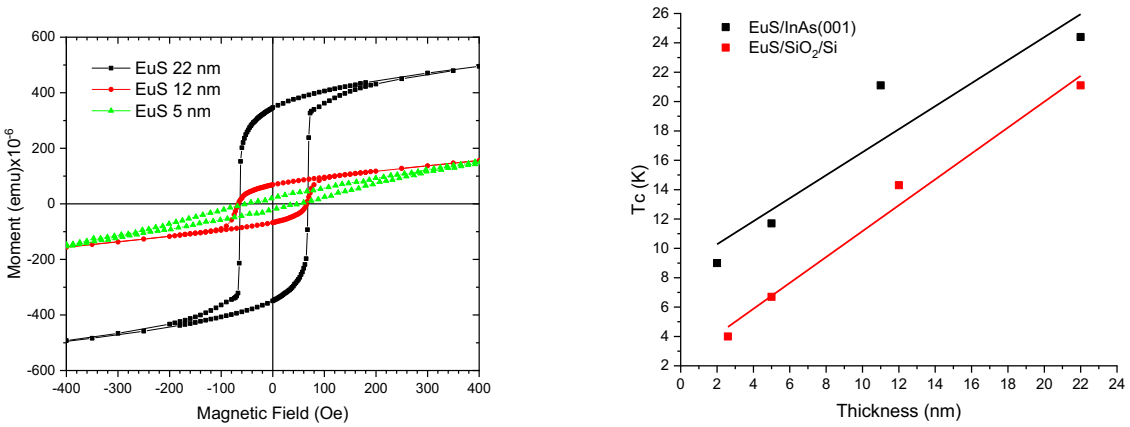

Figure 3: Magnetization loops measured for Al(16nm)/EuS(xx)/InAs(001) and T_C as a function of the thickness of the EuS layer for both Se/EuS xx/SiO$_2$/Si and Al(16nm)/EuS(xx)/InAs(001) samples.

Similar results have been obtained for the series of the EuS films (grown at RT) on the oxidized silicon wafers. Although FMR data are not available, magnetization loops shown in the left panel of Fig. 3 clearly demonstrate decreasing of the saturation magnetization with decreasing of the thickness of EuS films. T_C plotted in the right panel of Fig. 3 for both series of samples has a similar trend but the curve corresponding to EuS/SiO$_2$/Si is systematically shifted to the lower values. Most probably it is the presence of the Eu^{3+} ions with a low magnetic moment that further decreases T_C in the non-epitaxial EuS films.

This project has received funding from the European Union's Horizon 2020 research and innovation programme under grant agreement No 800923.

Table 1: Parameters of the epitaxial EuS/InAs(001) films

Sample composition	Curie Temperature (K)	Saturation magnetization 4π M (kG)
Al 16 nm/EuS 2nm/InAs(001)	9	NA
Al 16 nm/EuS 5nm/InAs(001)	11.7	6.6
Al 16 nm/EuS 11nm/InAs(001)	21.1	10.4
Al 16 nm/EuS 23nm/InAs(001)	24.4	15.2

3. Magnetic and magnetoelectric properties of the Al/EuS – based tunnel junctions

Although the characterization of bilayer systems is very useful for academic purposes, our aim in the SUPERTED project is to fabricate a micro-patterned tunnel junction structure. Therefore, in WP 1, we strive to design and implement inside the UHV system all the capabilities to grow the patterned tunnel junctions. In particular, we design, install and test two new instrumentations. First, a new manipulator (designed by us) that allows the sequential growth of the multilayers using shadow masks. Second, we have acquired and installed an oxygen plasma source to grow the required Al_2O_3 tunnel junction. This last oxidation technique was commercially available and we have just adapted our experimental system to install it. However, the manipulator required for the growth of patterned multilayer devices was not a standard design. Next, we will explain it in detail, remarking the important parts and the first results obtained after implementation.

3.1 Implementation of the shadow mask patterning in the UHV growth chamber

As mentioned above, a new custom manipulator was designed and bought with SUPERTED funding to implement the required shadow mask patterning in the UHV chamber. Figure 4 shows sketches of the sample stage with a shadow mask. The combination of two masks allows for making crossed bars with contact pads comprising tunnel junctions. Three different sets of masks are manufactured for junctions with nominal width of the current leads of 300, 200, and 100 µm. In addition to implementing a shadow mask patterning, the manipulator also allows samples to be heated to 800 °C or cooled to liquid nitrogen temperature. The masks mounted on standard Omicron-type sample holders are compatible with standard means of the transferring within the UHV systems and do not require opening of the chamber for manipulation.

This project has received funding from the European Union's Horizon 2020 research and innovation programme under grant agreement No 800923.

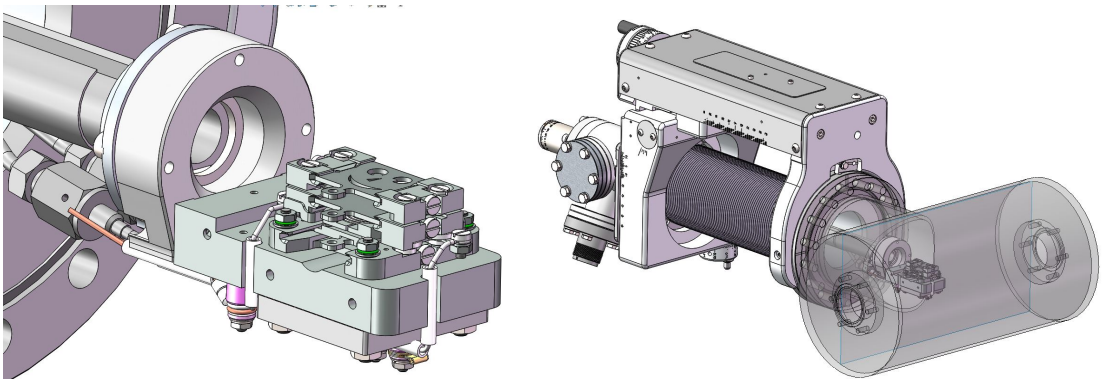

Figure 4: Close-up of sample stage with a shadow mask and sketch of the growth chamber with mounted manipulator

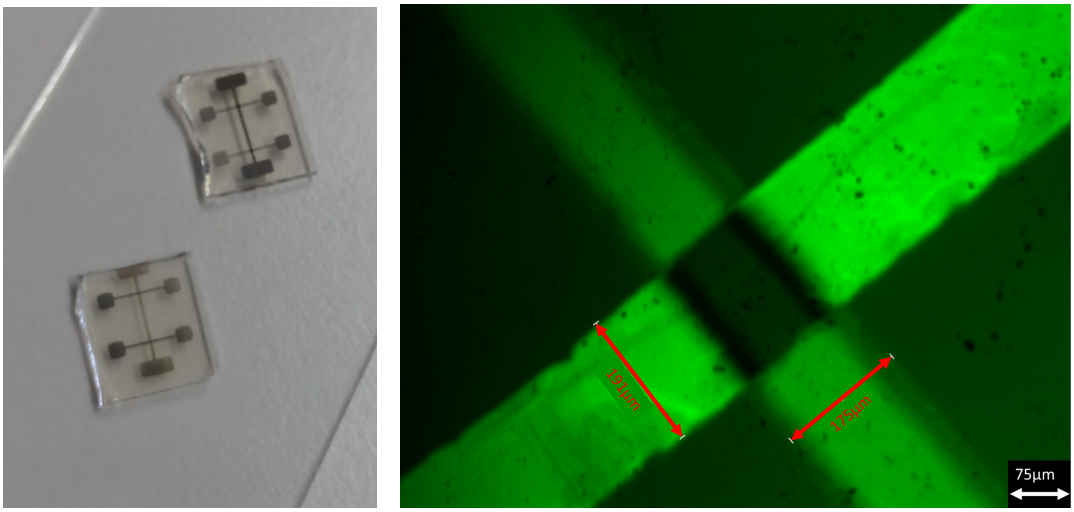

Figure 5: Examples of tunnel junctions with contact pads grown by shadow masking on glass substrates and the optical microscope image of the junction with nominal width of the wires of 200 µm.

Examples of the tunnel junctions made with the shadow mask patterning in our UHV system are shown in Fig. 5. In this case, Al crosses with nominal width of 200 µm were prepared on a polished glass substrate having a thickness of 500 µm. The optical microscope image demonstrates the sharp edges of the leads and proves the overall feasibility of the preparation of the patterned structures in the system. The growth chamber has six ports focused in the center of the sample stage (three on the top and three on the bottom). This allows mounting of various evaporators with different materials and a growth of the whole device in the same chamber. This design minimizes the amount of transfer, reduces risk of contamination and facilitates the overall growth process.

This project has received funding from the European Union's Horizon 2020 research and innovation programme under grant agreement No 800923.

3.2 Al/Al-Ox/Al/EuS tunnel junctions

Once all of this instrumentation was completed and with our experience of growing EuS and Al layers, we move to the next step, which was to fabricate patterned structures with two Al layers separated by an AlO_x barrier and grown on a EuS bias layer [3,6,7]. We try to demonstrate the reliability of the whole growth process and optimize its parameters. Over the past two months various tunnel junctions have been grown and their quality was found to be reproducible. In San Sebastian, we use a Quantum Design´s PPMS system to determine the resistance of the tunnel barriers. Further measurements to determine the spin-splitting DOS must be made at Pisa, because PPMS system cannot reach the temperature of the superconducting transition of Al.

An example of patterned multilayer systems is shown in Figure 6, where the sample was mounted on the resistivity measurements sample stage of the Quantum Design´s PPMS system. This $Al/AlO_x/Al/EuS/glass$ structure has the current leads with nominal width of 200 µm, both Al layers are 18 nm thick and the bottom EuS layer is 8 nm thick. In this case, the resistance of the longer and shorter leads are 68 Ω and 38 Ω, respectively. These values correspond to the resistivity of $3.5x10^{-6}$ ΩCm and $1.95x10^{-6}$ ΩCm, respectively, that are close to the reference value $2.65x10^{-6}$ ΩCm of the resistivity of a pure Al.

Figure 6: Al/AlOx/Al/EuS/glass structure mounted on the resistivity measurements sample stage of the Quantum Design´s PPMS system

This project has received funding from the European Union's Horizon 2020 research and innovation programme under grant agreement No 800923.

Figure 7 shows the first results of tunnel barrier resistance that we have obtained in an Al/AlO_x/Al/EuS/glass structure with four-point technique. As can be seen, the measurement yields negative resistance values. This known problem appears when the resistance of the barrier is lower than that of the leads [13]. Typical values of the area times resistance product for thin Al_2O_3 barriers are 10 to 10^3 Ωμm^2 [14]. Our structures, which are 200 μm wide, have area of the tunnel contact of $4x10^4$ μm^2, giving a resistance of $0.25x10^{-3}$ – $0.25x10^{-1}$ Ω. Figure 7 shows measurements of the temperature dependence of the barrier´s resistance. Resistance remains negative down to 10 K and therefore bare decreasing of temperature is not enough to overcome this problem. An ultimate solution is doing the measurements at a temperature below a superconducting transition of Al, in this case the residual resistance of the leads will be lower than resistance of the barrier and the negative resistance error will not distort the results.

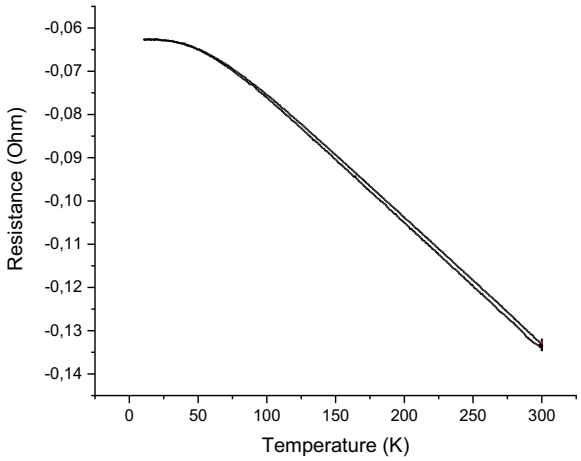

Figure 7: Temperature dependence of the resistance of the barrier in the Al/AlOx/Al/EuS/glass structure measured by a four-point technique.

4. Main results and conclusions

During this first 12 months of the project, we have followed the proposed work plan, both by controlling the multilayer growth of Al/EuS systems and by installing an experimental set up for patterned growth. By studying the Al/EuS bilayer system, we have determined systematic variations in the magnetic properties of both epitaxial and non-epitaxial EuS films as a function of the growth parameters. Monotonic decrease of Ms with the thickness of the EuS films should have a repercussion in the strength of the exchange coupling between the EuS and Al. Therefore, thickness can be considered as an optimization parameter for tuning the value of the spin-dependent splitting of the electronic DOS of a superconductor. The value of the effective field inversely depends on the thickness of the superconducting layer, and it can also serve as an additional degree of freedom in the optimization process. In addition, T_C changes in a similar way as the saturation magnetization and can be used to estimate the respective value of the Ms. Despite reduced values of T_C, all studied

This project has received funding from the European Union's Horizon 2020 research and innovation programme under grant agreement No 800923.

samples possess a large remanence that allows for a zero-field spin-split DOS of the Al (still has to be confirmed by tunneling spectroscopy).

The shadow mask technique has been implemented in the growth chamber, and the feasibility of growth of the patterned tunnel junctions has been demonstrated. Characterization of the metallic leads shows that Al is clean and has a resistivity close to the nominal value. The characterization of the tunnel barrier and the effect of the EuS layer on the Al must be studied further in the mK cryostat in Pisa, Italy.

4.1 Timetable for the next year

Since the technical requirements we needed for our new manipulator were not commercially available, the design, construction and installation of this new manipulator took the first 6 months of the project. This has led to a slight delay of about one month in the work plan. We are currently ready to manufacture patterned multilayer devices, and we are beginning to characterize their spin-splitting DOS. Since these measurements must be made in Pisa, Italy, we are now arranging a sample deliverable schedule for the regular delivery/characterization of the samples. Currently, we have fabricated the first set of samples with two Al leads and we plan to grow the samples with Co over the next month.

The work plan for the next 12 months includes:

- Fabrication and optimization of patterned multilayer devices in different conditions to optimize the spin-splitting DOS. This includes the shipment to Pisa (6 months). These are Tasks 1.2-1.5 in the work plan.
- Characterization of "*in situ*" growth of ferromagnetic insulators/superconductors beyond EuS/Al (12 months). As a starting point we will study a combination of GdN/TiN as mentioned in the Task 1.6.

This project has received funding from the European Union's Horizon 2020 research and innovation programme under grant agreement No 800923.

Bibliography

[1] A. Ozaeta, P. Virtanen, F. S. Bergeret, T. T. Heikkilä, Phys. Rev. Lett. 112, 057001 (2014)

[2] S. Kolenda, C. Sürgers, G. Fischer, D. Beckmann, Phys. Rev. B 95, 224505 (2017)

[3] E. Strambini, V. N. Golovach, G. De Simoni, J. S. Moodera, F. S. Bergeret, F. Giazotto, Phys. Rev. Materials 1, 054402 (2017)

[4] Y. M. Xiong, S. Stadler, P.W. Adams, G. Catelani, Phys. Rev. Lett. 106, 247001 (2011)

[5] R. Meservey and P.M. Tedrow, Phys. Rep. 238, 173—243 (1994)

[6] X. Hao, J. S. Moodera, R. Meservey, Phys. Rev. Lett. 67, 1342 (1991)

[7] X. Hao, J. S. Moodera, R. Meservey, Phys. Rev. B 42, 8235 (1990)

[8] A. Mauger and C. Godart, Phys. Rep. 141, 51 (1986)

[9] C. J. P. Smits, A. T. Filip, J. T. Kohlhepp, H. J. M. Swagten, B. Koopmans, W. J. M. de Jonge, Journ. App. Phys. 95, 7405 (2004)

[10] Guo-Xing Miao and Jagadeesh S. Moodera, Appl. Phys. Lett. 94, 182504 (2009)

[11] A. Goschew, J. Griesmar, P. Fumagalli Thin Solid Films 625, 106–110 (2017)

[12] S. Demokritov, U. Rticker, P. Grtinberg Journal of Magnetism and Magnetic Materials 163, 21-26 (1996)

[13] J. M. Pomeroy, H. Grube J. Appl. Phys., 105, 094503 (2009)

[14] H. Boeve, J. De Boeck, G. Borghs, J. Appl. Phys., 89,482, (2001)

This project has received funding from the European Union's Horizon 2020 research and innovation programme under grant agreement No 800923.